0090-9556/97/2512-1395–1406$02.00/0
DRUG METABOLISM AND DISPOSITION

Vol. 25, No. 12
Printed in U.S.A.

METABOLISM AND EXCRETION OF A NEW ANTIANXIETY DRUG CANDIDATE, CP-93,393, IN CYNOMOLGUS MONKEYS

Identification of the novel pyrimidine ring cleaved metabolites

CHANDRA PRAKASH AND DONGHUI CUI

Department of Drug Metabolism, Central Research Division, Pfizer Inc.

(Received June 24, 1997; accepted September 9, 1997)

ABSTRACT:

The metabolism and excretion of a new anxiolytic/antidepressant drug candidate, CP-93,393, {(7S,9aS)-1-(2-pyrimidin-2-yl-octahydro-pyrido[1,2-a]-pyrazin-7-yl-methyl)-pyrrolidine-2,5-dione} were investigated in cynomolgus monkeys after oral administration of a single 5 mg/kg dose of ^{14}C-CP-93,393. Urine, bile, feces, and blood samples were collected and assayed for total radioactivity, parent drug, and metabolites. Total recovery of the administered dose after 6 days was 80% with the majority recovered during the first 48 hr. An average of 69% of the total radioactivity was recovered in urine, 4% in bile, and 7% in feces. Mean C_{max} and $AUC_{(0-\infty)}$ values for the unchanged CP-93,393 were 143.2 ng/ml and 497.7 ng·hr/ml, respectively, in the male monkeys and 17.2 ng/ml and 13.7 ng·hr/ml, respectively, in the female monkeys.

HPLC analysis of urine, bile, feces, and plasma from both male and female monkeys indicated extensive metabolism of CP-93,393 to several metabolites. The identification of metabolites was achieved by chemical derivatization, β-glucuronidase/sulfatase treatment, and by LC/MS/MS, and the quantity of each metabolite was determined by radioactivity detector. CP-93,393 undergoes metabolism by three primary pathways, aromatic hydroxylation, oxidative degradation of the pyrimidine ring, and hydrolysis of the succinimide ring followed by a variety of secondary pathways, such as oxidation, methylation, and conjugation with glucuronic acid and sulfuric acid. The major metabolites, oxidation on the pyrimidine ring to form 5-OH-CP-93,393 (M15) followed by glucuronide and sulfate conjugation (M7 and M13), accounted for 35–45% of the dose in excreta. Two metabolites (M25 and M26) were formed by further oxidation of M15 followed by methylation of the resulting catechol intermediate presumably by catechol-*O*-methyl transferase. A novel metabolic pathway, resulting in the cleavage of the pyrimidine ring, was also identified. The metabolites (M18, M20, and M21) observed from this pathway accounted for 8–15% of the dose. Aliphatic hydroxylation of the succinimide ring was a very minor pathway in monkey. 5-Hydroxy-CP-93,393 (M15, 37–49%), its sulfate and glucuronide conjugates (M7 and M13, ~34%), and the pyrimidine ring cleaved product (M18, ~8%) were the major metabolites in monkey plasma. The identified metabolites accounted for approximately 90, 93, 97, and 92% of the total radioactivity present in urine, bile, plasma, and feces, respectively. The major *in vivo* oxidative metabolites were also observed after *in vitro* incubations with monkey liver microsomes.

CP-93,393, {(7S, 9aS)-1-(2-pyrimidin-2-yl)-octahydro-pyrido[1,2-a]pyrazin-7-yl-methyl)-pyrrolidine-2,5-dione, fig. 1}, is a novel anxiolytic/antidepressant drug candidate that exhibits highly selective serotonin 5-HT1A[1] autoreceptor agonist activity and potent antagonist activity at the human α2 adrenergic receptor (1–4). It lacks affinity for benzodiazepine receptors and, therefore, is not likely to have the sedative and addictive properties of diazepam or alprazolam (5, 6). CP-93,393 is well tolerated in animals at doses anticipated to be clinically efficacious. Pharmacokinetic studies of orally administered CP-93,393 in rats and monkeys suggested that it is rapidly absorbed with T_{max} of 1 hr in both rats and monkeys.[2] After iv administration to rats and monkeys, the elimination half lives ($t_{1/2}$) of CP-93,393 ranged from 0.3 to 0.5 hr. In addition, extensive first-pass metabolism of CP-93,393 occurred after oral administration resulting in bioavailabilty ranging from 4 to 15%.[2] The major metabolic pathways in rats involved hydroxylation at the pyrimidine and succinimide rings followed by conjugation with glucuronic acid and sulfuric acid (7). Preliminary *in vitro* studies using hepatic subcellular fractions from rat and human also indicated that CP-93,393 is metabolized predominantly by hydroxylation on the pyrimidine ring (8).

To understand the metabolic fate of CP-93,393 in cynomolgus monkey, one of the primary species used in preclinical safety evaluations, metabolism studies were conducted by oral administration of ^{14}C-CP-93,393 to conscious bile-cannulated cynomolgus monkeys. This report describes the results observed from the analysis of urine, bile, feces, and plasma, revealing information about extent of absorption, routes of elimination, and metabolism for this new anxiolytic

[1] Abbreviations used are: 5-HT, 5-hydroxytryptamine; 5-OH-CP-93,393, 1-[2-(5-hydroxy-pyrimidin-2-yl)-octahydro-pyrido[1,2-a]pyrazin-7-ylmethyl]-pyrrolidine-2,5-dione; CP-93,558, (2-pyrimidin-2-yl-octahydro-pyrido[1,2-a]pyrazin-7-yl)-methylamine; radio-HPLC, HPLC with on-line radioactivity detector; CP-123,974 (2-OH-CP-93,393), 3-hydroxy-1-(2-pyrimidin-2-yl-octahydro-pyrido[1,2-a]pyrazin-7-yl-methyl)-pyrrolidine-2,5-dione; NPMSA, 1-(2-pyrimidin-2-yl-octahydro-pyrido[1,2-a]pyrazin-7-ylmethyl)-succinamic acid; 2-NPMHSA, 1-(2-pyrimidin-2-yl-octahydro-pyrido[1,2-a]pyrazin-7-ylmethyl)-2-hydroxy-succinamic acid; 3-NPMHSA, 1-(2-pyrimidin-2-yl-octahydro-pyrido[1,2-a]pyrazin-7-ylmethyl)-3-hydroxy-succinamic acid; 5-NHPMSA, 1-[2-(5-hydroxy-pyrimidin-2-yl)-octahydro-pyrido[1,2-a]pyrazin-7-ylmethyl]-succinamic acid; β-RAM, radioactive monitor; CAD, collisionally activated dissociation; MRM, multiple reaction monitoring, SIM, selected ion monitoring.

Send reprint requests to: Dr. Chandra Prakash, Department of Drug Metabolism, Central Research Division, Pfizer Inc., Groton, CT 06340.

[2] J. Baxter, *et al.* Manuscript in preparation.

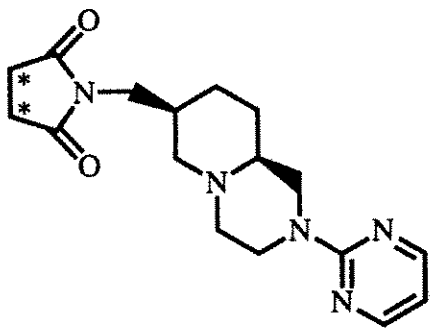

FIG. 1. *Structure of ^{14}C-CP-93,393.*

drug. The metabolites were quantitated by radio-HPLC, and were characterized by LC/MS, β-glucuronidase/sulfatase treatment, and by chemical derivatization. The structures of several metabolites were confirmed by comparisons of their HPLC retention times with synthetic standards and metabolites obtained from *in vitro* incubations with monkey liver microsomes.

Materials and Methods

General Chemicals. Commercially obtained chemicals and solvents were of HPLC or analytical grade. β-Glucuronidase (from Helix Pomatia, type H-1 with sulfatase activity), $NADP^+$, DL-isocitric acid, and isocitric dehydrogenase were obtained from Sigma Chemical Co. (St. Louis, MO). YMC basic columns were obtained from YMC (Wilmington, NC). Ecolite (+) scintillation cocktail was obtained from ICN (Irvine, CA). Carbosorb and Permafluor V scintillation cocktails were purchased from Packard Instrument Co. (Downers Grove, IL). Hexafluoroacetylacetone was obtained from Aldrich Chemical Co. (Milwaukee, WI).

Radiolabeled Drug and Reference Compounds. ^{14}C-CP-93,393 (HCl salt), labeled at C-2 and C-3 positions of the succinimide ring, 5-hydroxy-CP-93,393 and CP-93,558 were synthesized at Pfizer Central Research (Groton, CT). ^{14}C-CP-93,393 showed a specific activity of 4.76 mCi/mmol (12.9 μCi/mg) and a radiochemical purity of ≥98% as determined by radio-HPLC. CP-123,974 (2-hydroxy-CP-93,393) was synthesized by the condensation of CP-93,558 with malic acid as described (9). NPMSA, 2-NPMHSA, 3-NPMHSA and 5-NHPMSA were prepared using the published procedures (10).

Animals and Dose Administration. All studies were conducted according to protocols approved by the Pfizer Animal Care and Use Committee. The cynomolgus monkeys (3.8–5.7 kg) were obtained from stock animals maintained at Pfizer Central Research and were placed in individual stainless-steel metabolism cages. The animals were fasted for 12 hr prior to the dose administration and were fed 4 hr after the dose. The dosing solution was prepared by dissolving ^{14}C-CP-93,393 in de-ionized water at a concentration of 2 mg/ml.

A group of two male and two female monkeys were given a single oral (gavage) dose of ^{14}C-CP-93,393 (5 mg/kg) for blood collection. Blood was collected in heparinized tubes from the femoral vein from each animal at 0, 0.25, 0.5, 1, 2, 3, 4, 8, 12, 24, and 48 hr after the dose. The blood samples were centrifuged and plasma was transferred to clean tubes.

Another group of male (N = 2) and female (N = 1) monkeys were surgically implanted with a skin button with tubing to the gall bladder and intestine that allows the continuous collection or re-circulation of bile. The animals were orally administered a 5 mg/kg dose of ^{14}C-CP-93,393. Total urine, bile, and feces were collected from 0–8, 8–24, 24–48, 48–72, 72–96, 96–120, and 120–144 hr after the dose. The first fecal sample was collected at 0–24 hr after the dose. Bile was collected in 250 ml plastic bottle containing 1 ml ammonium acetate (1 M, pH 5.5) to avoid hydrolysis of the drug and its metabolites. The biological samples were kept at −20°C until analyzed.

Determination of Radioactivity. The radioactivity in urine, bile, and plasma was determined by liquid scintillation counting. Aliquots of plasma, urine, and bile (50 μl, each) were mixed with 5 ml of Ecolite (+) scintillation cocktail and counted in a Packard #2500 TR liquid scintillation counter (Downers Grove, IL). Fecal samples were placed in Stomacher 400 bags and homogenized in water to a thick slurry using a Stomacher 400 Lab Blender (Cooke Laboratory Products, Alexandria, VA). Aliquots (~500 mg) of the homogenates were air dried over night and combusted using a Packard Tricarb Oxidizer model 307. The liberated $^{14}CO_2$ was trapped in Carbosorb and Permafluor V and the radioactivity in the trapped samples was determined by counting in the liquid scintillation counter. Combustion efficiencies were determined by combustion of ^{14}C-standards in an identical manner. The samples obtained at 0 hr after the dose were used as controls and counted to obtain background count rate.

The amount of radioactivity in the dose was defined as 100% and the radioactivity in urine, bile, and feces at each sampling time was expressed as the percentage of dose excreted in the respective matrices at that sampling time. The amount of radioactivity in plasma was expressed as ng-equiv of parent drug/ml and was calculated by using the specific activity of the dose administered.

Pharmacokinetic Analysis. Plasma concentrations of unchanged CP-93,393 were determined by a standard HPLC/MS/MS assay (11). Pharmacokinetic parameters were determined using a conventional method (12). Values of C_{max} and T_{max} were assessed by visual inspection. The elimination rate constants (k) and terminal plasma $t_{1/2}$ were derived by log-linear least squares regression of the profiles. The values of AUCs were calculated up to the last detectable concentration time point t by the trapezoidal rule and were extrapolated to infinity using elimination rate constants (k). The T_{max} value was the time of the first occurrence of the maximal plasma concentration (C_{max}).

Extraction of Metabolites from Biological Samples. Urine and bile samples collected from 0–8 and 8–24 hr after the dose were pooled on the basis of ratios of the total volumes collected at those time intervals. The pooled urine (~1 ml) was centrifuged and an aliquot of the supernatant was injected into the HPLC without further purification. Pooled bile and plasma (0–24 hr, 0.5 ml from each time point) samples were diluted with four volumes of acetonitrile and the precipitated material was removed by centrifugation. The pellets were washed with an additional one volume of acetonitrile and both supernatants were combined. Small aliquots of supernatants and pellets were counted to determine the extraction recovery. The supernatant was evaporated to dryness on a Speed Vac evaporator (Savant Instruments, NY) and reconstituted in HPLC mobile phase.

The fecal homogenate (~12 g, 0–24 hr) was diluted with methanol (60 ml). The suspension was stirred overnight on a magnetic stirrer and centrifuged. The pellet was washed with an additional 10 ml of methanol and both supernatants were combined. A small aliquot of supernatant was counted to determine the extraction recovery. The supernatants were evaporated on a Speed Vac evaporator and the residue was dissolved in 600 μl of HPLC mobile phase and an aliquot (80 μl) was injected into the LC/MS.

Derivatization. An aliquot of the extracted bile sample (100 μl) was suspended in 500 μl of saturated sodium bicarbonate solution. Hexafluoroacetylacetone (50 μl) in toluene (500 μl) was then added and the reaction mixture was heated at about 90°C for 2 hr (13). The solvents were evaporated on a Speed Vac evaporator and the residue was reconstituted in HPLC mobile phase and analyzed by LC/MS.

Enzymatic Hydrolysis. Urine samples (0.5 ml each) were adjusted to pH 5 with sodium acetate buffer (0.1 M) and treated with 2,000 units of β-glucuronidase/sulfatase. The mixture was incubated in a shaking water bath at 37°C for 12 hr and was then diluted with acetonitrile. The precipitated protein was removed by centrifugation. The pellet was washed with an additional 2 ml of acetonitrile and the two supernatants were combined. The supernatant was concentrated and dissolved in 0.5 ml of HPLC mobile phase, and an aliquot (80 μl) was injected into the HPLC system. Incubation of urine samples for 12 hr without the enzyme served as a control.

***In Vitro* Incubations.** Monkey liver microsomes were prepared by differential centrifugation using standard procedures (14). Protein concentrations were measured by the bicinchoninic acid assay using crystalline bovine serum albumin as standard (15) and CYP concentrations were determined by the method of Omura and Sato (16). The incubation mixture (final volume 1 ml) contained liver microsomes (0.5 μM CYP), ^{14}C-CP-93,393 (20 μM), 100 mM

TABLE 1

Percentage of administered radioactivity recovered in urine, bile, and feces of monkeys at different intervals

Monkeys #	0–8 hr	8–24 hr*	24–48 hr	48–72 hr	72–96 hr	96–120 hr	120–144 hr	Total
Female 1								
Urine	69.50	8.82	1.04	0.47	0.15	0.08	0.09	80.2
Bile	4.99	0.96	0.11	0.03	0.00	0.00	0.00	6.1
Feces	—	1.74	0.35	0.09	0.16	—	0.02	2.4
Total	74.49	11.52	1.5	0.59	0.31	0.08	0.11	88.6
Male 1								
Urine	47.47	21.1	1.15	0.53	0.26	0.17	0.07	70.8
Bile	0.06	0.29	0.39	0.00	0.01	0.02	0.03	0.8
Feces	—	9.18	0.64	0.05	0.22	0.05	0.02	10.2
Total	47.53	30.57	2.18	0.58	0.49	0.24	0.12	81.7
Male 2								
Urine	24.63	18.26	2.46	0.49	0.29	0.11	0.07	46.3
Bile	2.50	0.41	0.60	0.05	0.00	0.00	0.00	3.6
Feces	—	8.03	3.09	0.76	0.28	0.01	0.01	12.2
Total	27.13	26.7	6.15	1.30	0.57	0.12	0.08	62.1
Mean Male	37.33	28.64	4.17	0.94	0.53	0.18	0.1	71.9

* Feces were from 0–24 hr.

potassium phosphate buffer (pH 7.4), and a NADPH-generating system (9 mM $MgCl_2$, 0.54 mM $NADP^+$, 6.2 mM DL-isocitric acid, and 0.5 U/ml isocitric dehydrogenase). The reactions were initiated by addition of a NADPH regenerating system after a 5-min preincubation period. Reactions were incubated at 37°C for 30 min and were stopped by addition of methanol (2 ml). The mixture was centrifuged and the supernatant was separated. The organic extract was evaporated and reconstituted for analysis by HPLC.

HPLC. HPLC was conducted on a system that consisted of a Rheodyne injector for manual injections, a LDC/Milton Roy constametric CM4100 gradient pump (Riviera Beach, FL), a Waters Lambda-Max model 481 UV detector (Milford, MA), a radioactivity monitor (β-RAM, INUS, Tampa, FL) and a SP 4200 computing integrator (Riviera Beach, FL). Chromatography was performed on a YMC basic HPLC column (4.6 mm × 250 mm, 5 μm) with a binary mixture of 20 mM ammonium acetate (solvent A) and acetonitrile (solvent B) at a flow rate of 1 ml/min. The mobile phase initially composed of solvent A/solvent B (95:5) for 10 min. It was then linearly programmed to solvent A/solvent B at 60:40 over a period of 25 min. Chromatography was performed under isocratic conditions for 10 min and then programmed back to the starting solvent mixture over a period of 10 min. The system was allowed to equilibrate for approximately 10 min before the next injection was made. The retention times of the radioactive peaks were compared with those of the synthetic standards.

Quantitative Assessment of Metabolite Excretion. Quantification of the metabolites was carried out by measuring radioactivity in the individual peaks that were separated on HPLC using a β-RAM. The β-RAM provided an integrated printout in cpm and percentage of radiolabeled material, as well as, peak representation. The β-RAM was operated in the homogeneous liquid scintillation counting mode with addition of 4 ml/min Ecolite (+) scintillation cocktail to the HPLC effluent after UV detection. The radio chromatograms of metabolites in plasma were generated by collecting fractions at 20 sec intervals and counting the fractions in a Packard #2200CA liquid scintillation counter. The retention time of radioactive peaks, where possible, were compared with synthetic standards and/or metabolites obtained from rat urine (7).

LC/MS. LC/MS was conducted on a Perkin-Elmer (PE) SCIEX API III$^+$ triple-stage quadrupole instrument equipped with an ion spray interface (Toronto, Ontario, Canada). The effluent from the HPLC column was split and about 50 μl/min was introduced into the atmospheric ionization source. The remaining effluent was directed into the flow cell of the β-RAM. The β-RAM response was recorded in real time by the mass spectrometer which provided simultaneous detection of radioactivity and MS data. The delay in response between the two detectors was about 0.2 min with the mass spectrometric response being recorded first. The ion spray interface was operated at 5500–5800 V and the mass spectrometer was operated in the positive ion mode. CAD studies were performed using argon gas at a collision energy of 25 eV and a collision gas thickness of 2.5×10^{14} molecules/cm^2. Data were processed with Qudra 950 Macintosh computer operating Mac-Spec software (PE-SCIEX; Toronto, Ontario, Canada).

Results

Excretion. The percentage of radioactivity excreted in urine, bile, and feces of male and female monkeys at different sampling times following oral administration of ^{14}C-CP-93,393 is shown in table 1. The total recoveries of the radioactivity in excreta were 88.6 and 71.9% for female and male monkeys, respectively. The recoveries of the radioactive material in urine, bile, and feces were 58.5, 2.2, 11.2% for male monkeys, and 80.2, 6.1, 2.4%, respectively, for a female monkey. Of all the radioactivity recovered in the urine, bile, and feces of monkeys, essentially all was recovered within 48 hr.

Metabolite Profiles in Urine, Bile, and Feces. The pooled bile and fecal samples were extracted and purified as described in the *Materials and Methods* section. The extraction recovery of the radioactivity was 87–92% from the bile and 62–67% from the feces. Radiolabeled components in urine, bile, and feces were analyzed for unchanged CP-93,393 and its metabolites by HPLC with flow-through radiochemical detection. The representative radio-HPLC profiles from urine, bile, and feces from a male monkey are shown in fig. 2. There were no significant gender-related qualitative differences in the profile from male and female monkeys. In addition to a small amount of unchanged CP-93,393, a total of 15 metabolites in urine, 11 metabolites in bile, and 13 metabolites in feces were detected. The percentages of metabolites excreted in relation to the total radioactivity in urine, bile, and feces are presented in table 2.

Identification of Excreted Metabolites. The structures of metabolites were elucidated by ion spray LC/MS using a combination of Q1 scan and product ion scanning techniques (7, 17, 18). Full scan (Q1) mass spectrum of CP-93,393 gave an abundant protonated molecular ion (MH^+) at *m/z* 330. CAD product ion spectrum (MS/MS) of *m/z* 330 provided a number of characteristic fragment ions (fig. 3). Cleavages across the piperazine moiety were the predominant dissociation processes with charge resides at both succinimide- and the pyrimidine-ring containing fragments. The fragmentation pattern proposed for CP-93,393 was substantiated by the mass spectra of structurally related compounds. Thus, the presence of ions at *m/z* 195, 209 and 235 were used to characterize the unchanged succinimide nucleus, while

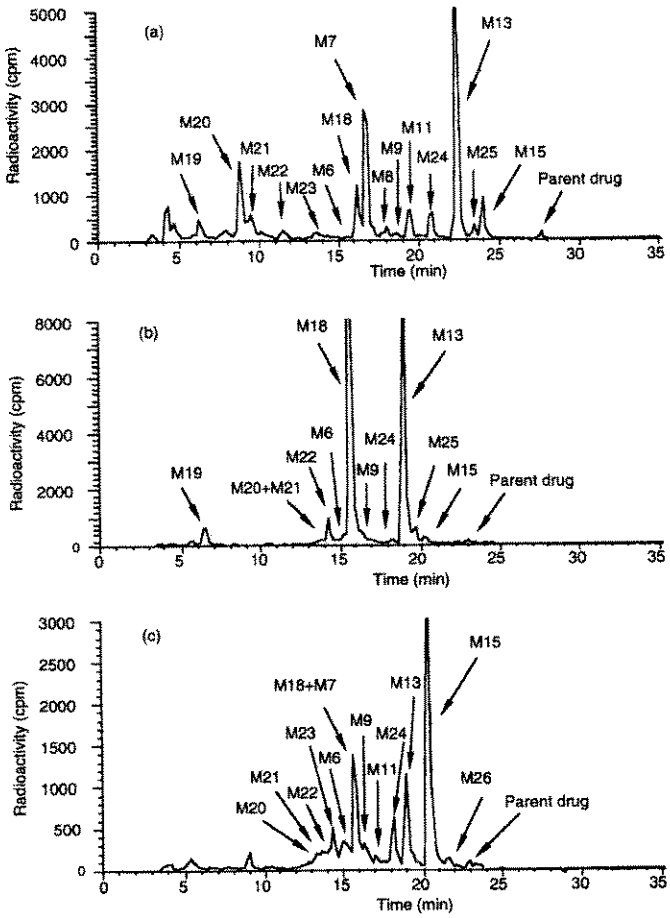

FIG. 2. *HPLC-radiochromatograms of CP-93,393 metabolites in monkey urine (A) bile (B) and feces (C).*

TABLE 2

Percentages of metabolites of CP-93,393 in urine, bile, and feces of monkeys after oral administration of ^{14}C-CP-93,393 at a dose of 5 mg/kg.

Metabolite	Retention Time (min:sec)	% of Recovered Radioactivity		
		Urine	Bile	Feces
M19	6:20	2.18	3.19	—
M20	8:52	11.01	1.28	2.36
M21	9:29	3.38	—	1.65
M22	10:11	1.95	3.61	0.91
M23	11:38	1.57	—	5.24
M6	13:37	2.57	0.90	6.00
M18	16:18	5.64	48.24	14.45
M7	16:50	11.42	1.65	—
M9	18:01	2.61	3.09	3.09
M8	18:48	1.38	—	—
M11	19:29	2.58	—	1.47
M24	20:52	2.89	1.18	6.23
M13	22:28	31.04	28.79	10.85
M25	23:33	1.19	2.72	0.35
M15	24:04	5.23	1.35	37.40
M26	25:22	—	—	1.68
Parent drug	27:42	3.49	0.64	0.64
		90.11	93.45	92.32

* Average of male and female monkeys.

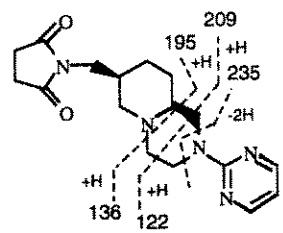

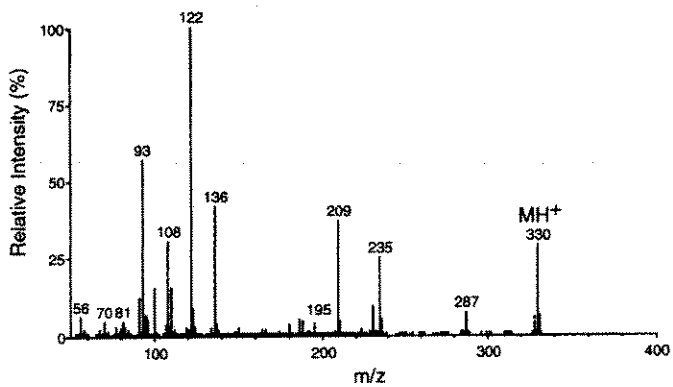

FIG. 3. *CAD product ion mass spectrum of CP-93,393.*

the mass shift of the ions at *m/z* 122 and 136 were used to monitor the change in the substituent(s) at the pyrimidine ring.

Metabolite M19. **M19** was detected in urine and bile. It had a retention time of 6:20 (min:sec) on HPLC and showed a protonated molecular ion at *m/z* 540. The CAD product ion spectrum of *m/z* 540 showed an ion at *m/z* 364, loss of 176 Da (characteristic loss of dehydroglucuronic acid) from the protonated molecular ion, indicating that **M19** was a glucuronic acid conjugate. Treatment of urine with β-glucuronidase resulted in the disappearance of **M19**, further suggesting that **M19** was a glucuronide conjugate. The ion at *m/z* 364, 34 Da higher than the parent drug, was indicative of the addition of an oxygen atom and a molecule of water to the parent molecule. The prominent ion at *m/z* 138, 16 Da higher than that of the parent drug, indicated that the oxidation had occurred at the pyrimidine ring. Based on these data, **M19** was tentatively identified as the glucuronide conjugate of 5-NHPMSA.

Metabolites M20 and **M21**. **M20** and **M21** had the retention times of 8:52 min and 9:29 min, respectively, on HPLC and were detected in urine, bile, and feces. Both **M20** and **M21** showed the same protonated molecular ion at *m/z* 382, suggesting that they were isomers. The MS/MS spectra of both **M20** and **M21** (*m/z* 382) gave prominent and significant ions at *m/z* 195, 209, 235, 252, 277, 294, 319, and 347 (fig. 4*A* and 4*B*). The ion at *m/z* 252 suggested the modification of the pyrimidine ring. The other prominent ions at *m/z* 195, 209, and 235 supported that the succinimide portion of the molecule was unsubstituted. The ion at *m/z* 319, loss of 63 Da, indicated the presence of a carboxyl and a hydroxyl group. The ion at *m/z* 347, loss of 35 Da (H_2O+NH_3), suggested the presence of a hydroxyl and an amino group. Based on these data, **M20** and **M21** were tentatively assigned as diastereoisomers of 3-{1-[7-(2,5-dioxo-pyrrolidin-1-yl-methyl)-octahydro-pyrido[1,2-a]pyrazin-2-yl]-vinyl-amino}-2-hydroxypropionic acid.

Metabolite M22. **M22** had a retention time of 10:11 min on HPLC and was present in all excreta. It exhibited a protonated molecular ion at *m/z* 444, 114 Da higher than the parent drug, suggesting that it was a conjugate. The MS/MS spectrum of *m/z* 444 gave an intense ion at

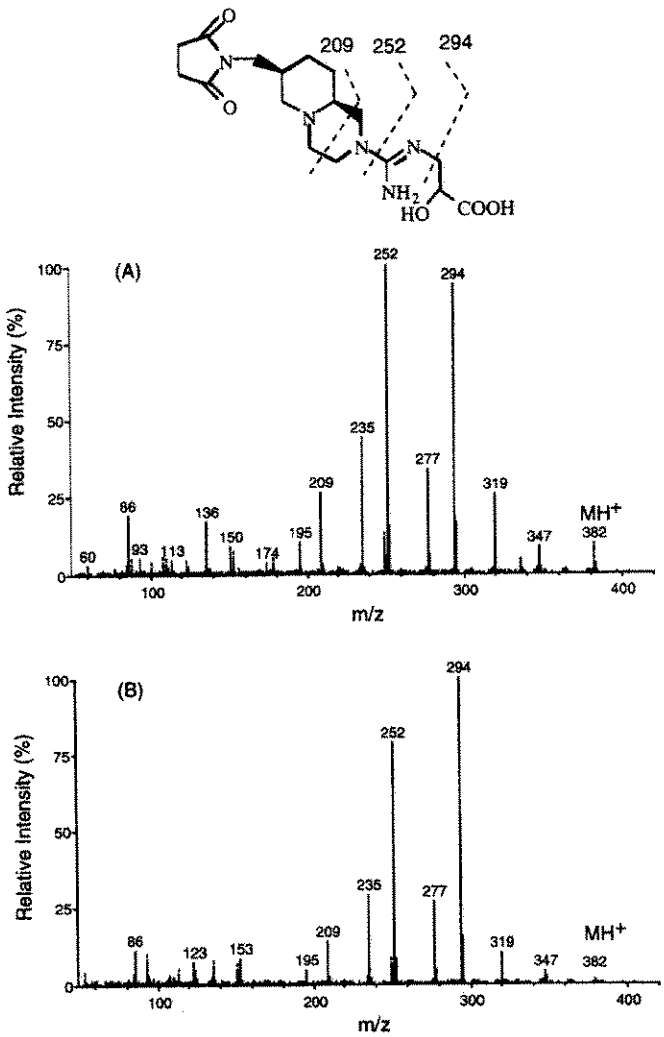

FIG. 4. *CAD product ion mass spectra of metabolite* **M20** (*A*) and **M21** (*B*) from urine.

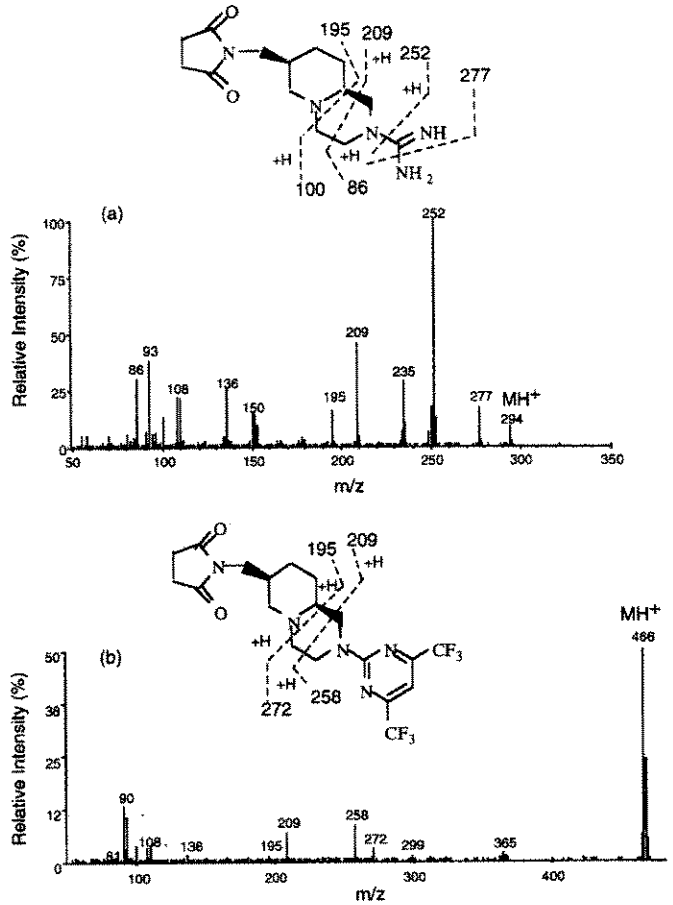

FIG. 5. *CAD product ion mass spectra of metabolite* **M18** (*A*) and its derivatized product (*B*) from bile.

m/z 364, loss of 80 Da (loss of SO_3) from the precursor ion, indicating that it was a sulfate conjugate. Treatment of urine with β-glucuronidase/aryl sulfatase resulted in the disappearance of **M22,** further suggesting that **M22** was a sulfate conjugate. The ion at *m/z* 364 further suggested the addition of an oxygen atom and a molecule of water to the parent molecule. The other characteristic ion at *m/z* 138 suggested the hydroxylation on the pyrimidine moiety. The ion at *m/z* 227 indicated that the addition of water had occurred at the succinimide ring. Based on these data, **M22** was tentatively identified as the sulfate conjugate of 5-NHPMSA.

Metabolite M23. **M23** had a retention time of 11:38 min on HPLC and was present in monkey urine and feces. It exhibited a protonated molecular ion at *m/z* 380, 50 Da higher than the parent drug, suggesting the addition of two oxygen atoms and a molecule of water. The CAD product ion spectrum of *m/z* 380 gave a characteristic fragment ion at *m/z* 138, suggesting that an oxygen atom had been added to the pyrimidine moiety. The significant ion at *m/z* 245, loss of 135 Da (succinamic acid + H_2O) from the parent ion, suggested that the addition of the other oxygen atom had occurred at the pyrido-pyrazinyl-methyl part of the molecule. The ion at *m/z* 306 suggested that the water molecule had been added at the succinimide ring. Based on these data, **M23** was tentatively identified as hydroxy-*N*-[2-(5-hydroxy-pyrimidin-2-yl)-octahydro-pyrido[1,2-a]pyrazin-7-yl]-methyl}-succinamic acid.

Metabolite M6. **M6** showed a protonated molecular ion at *m/z* 364, 34 Da higher than CP-93,393, suggesting the addition of an oxygen atom and a molecule of water. **M6** was identified as 5-NHPMSA by a comparison of its retention time on HPLC and CAD product ion spectrum with a synthetic standard.

Metabolite M18. **M18** had a retention time of 16:18 min on HPLC and was present in all excreta. It showed a protonated molecular ion at *m/z* 294, lower than that of the parent drug, suggesting that it was a cleaved product. The CAD product ion spectrum of **M18** gave abundant ions at *m/z* 252, 235, 209, and 195 (fig. 5A). The fragment ion at *m/z* 252, loss of 42 Da from the molecular ion, suggested the presence of an acetyl or a carboxamidino group. The other prominent ions at *m/z*, 209 and 235, suggested that the succinimide portion of the molecule was unsubstituted.

Treatment of bile with hexafluoroacetylacetone resulted in the disappearance of peak coinciding with metabolite **M18** and appearance of a new peak that had the retention time of 38:48 min on HPLC. It showed a protonated molecular ion at *m/z* 466, 172 Da higher than the underivatized compound, indicative of an addition of hexafluoroacetylacetone moiety with subsequent loss of two molecules of water (fig. 5*B*). The MS/MS spectrum of *m/z* 466 gave abundant ions at *m/z* 272, 258, 209, and 195. The diagnostic ions at *m/z* 195 and 209 indicated that the succinimide moiety was unaltered. The fragment

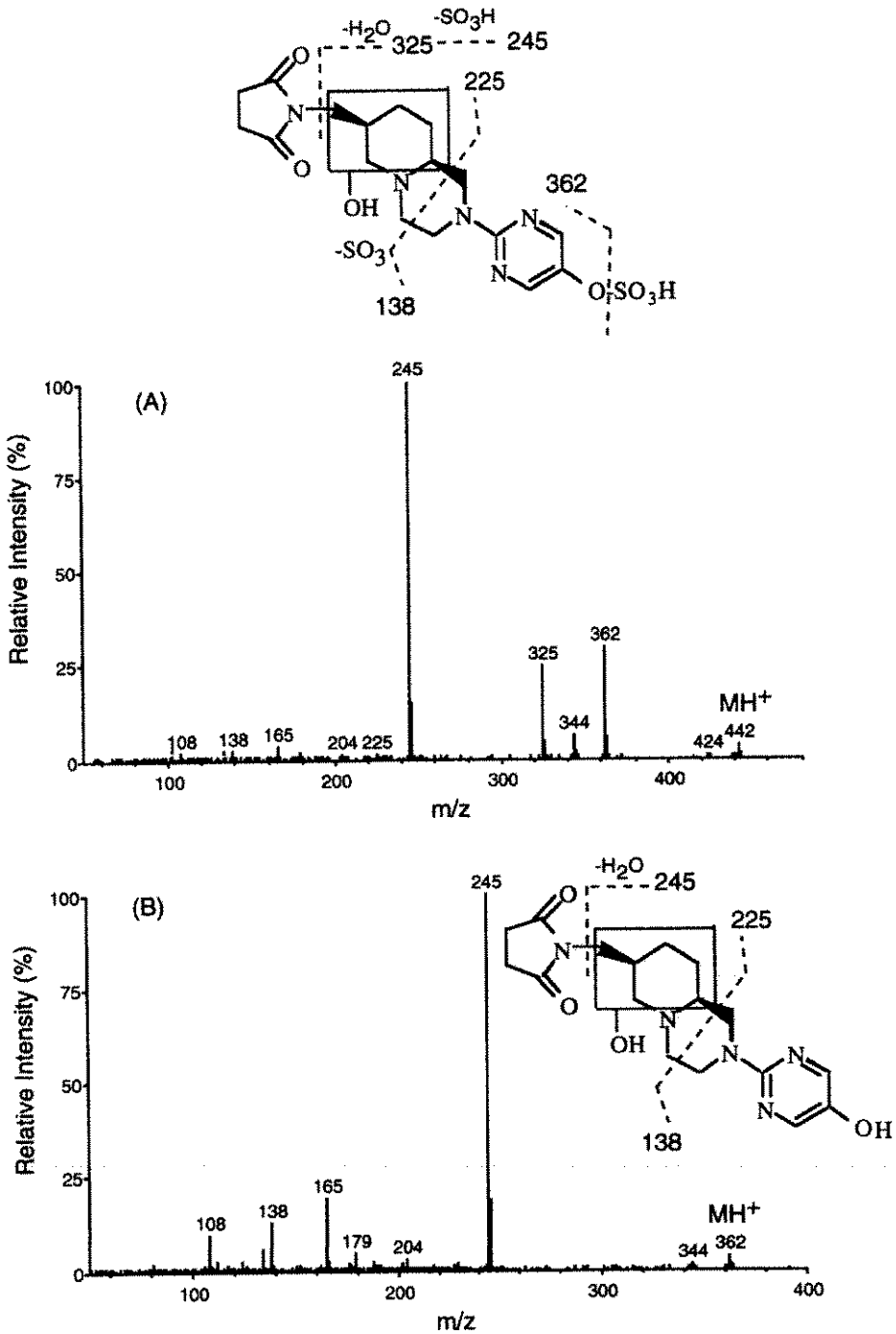

FIG. 6. *CAD product ion mass spectra of metabolite* **M11** (*A*) and **M24** (*B*) from urine.

ions at *m/z* 272 and 258, 136 Da higher than those of the parent drug, suggested the addition of two trifluoromethyl groups at the pyrimidine ring. On the basis of these data, **M18** was tentatively identified as 7-(2,5-dioxo-pyrrolidin-1-yl-methyl)-octahydro-pyrido[1,2-a]pyrazine-2-carboxamidine.

Metabolite M7. **M7** had a retention time of 16:50 min on HPLC and was present in all excreta. It displayed a protonated molecular ion at *m/z* 522, 192 Da higher than the parent drug, indicating that it was a glucuronide conjugate of the hydroxylated metabolite. The ion at *m/z* 138 in the MS/MS spectrum of **M7** suggested the presence of a hydroxyl group on the pyrimidine ring. Treatment of the urine sample with β-glucuronidase/aryl sulfatase resulted in the disappearance of **M7** and the increase in peak area of **M15**. Based on these data, **M7** was identified as the glucuronide conjugate of **M15**.

Metabolite M9. M9 had a retention time of 18:01 min on HPLC and was found in urine, feces, and bile. It showed a protonated molecular ion at *m/z* 348, 18 Da higher than the parent drug, suggesting that the molecule had undergone hydrolysis. **M9** had similar retention time as synthetic NPMSA standard on HPLC. **M9** was thus identified as NPMSA.

Metabolite M8. **M8** had a retention time of 18:48 min on HPLC and was present only in urine. It showed a protonated molecular ion at *m/z* 364, 34 Da higher than the drug, indicative of the addition of an oxygen atom and a molecule of water. The fragment ion at *m/z* 318,

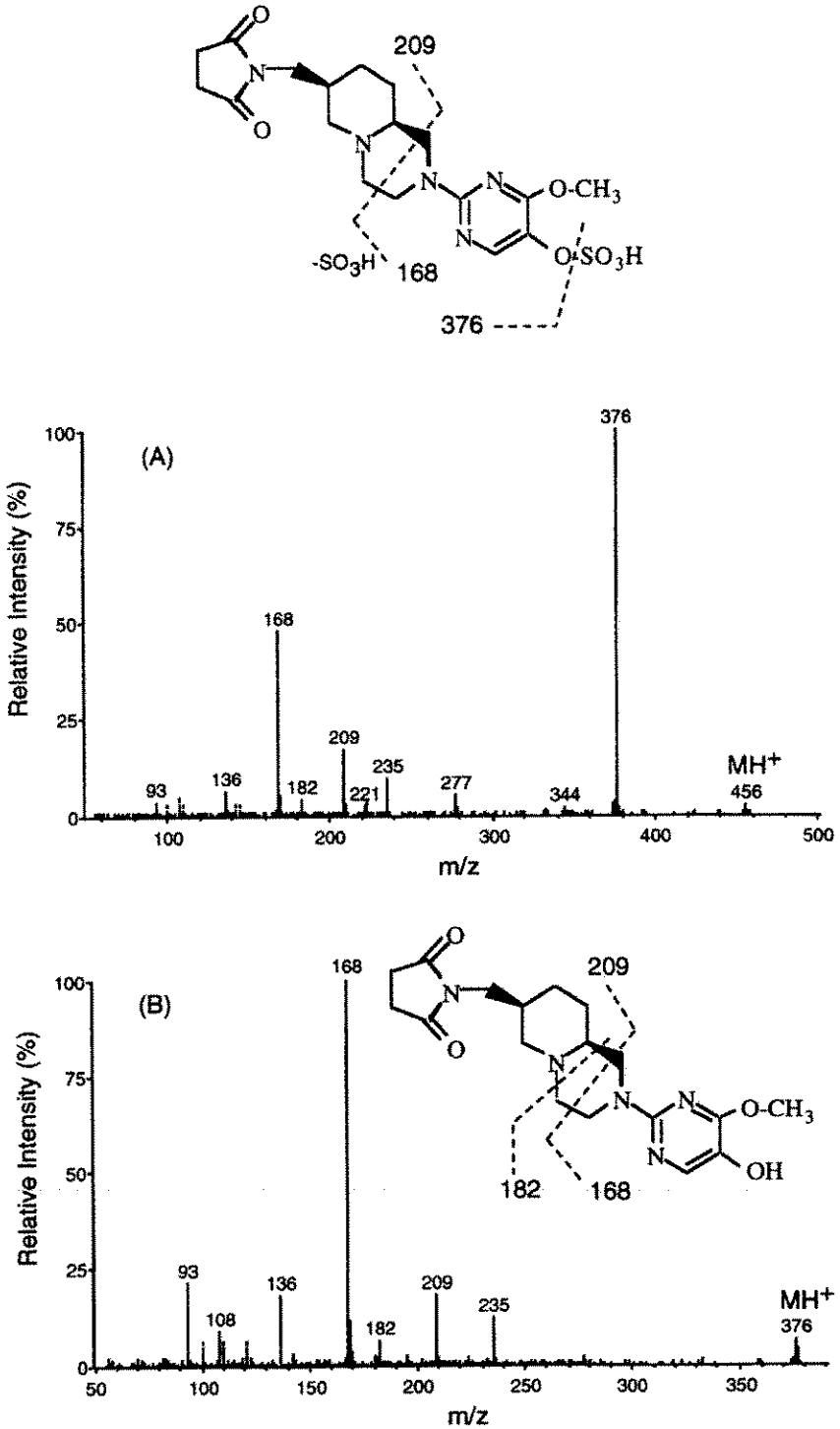

FIG. 7. *CAD product ion mass spectra of metabolite* **M25** (*A*) and **M26** (*B*) from urine.

loss of 46 Da in its CAD spectrum, suggested the presence of a free -COOH group. The presence of other fragment ions at *m/z* 231, 248, 136, and 122 suggested that the oxidation had occurred at the succinimide moiety. The ion at *m/z* 290 (loss of ·COHCOOH from the protonated molecular ion) indicated the position of hydroxyl group to be alpha to the carboxyl group. **M8** had a similar retention time on HPLC as was synthetic 2-NPMHSA. **M8** was thus identified as 2-NPMHSA.

Metabolite M11. **M11** had a retention time of 19:29 min on HPLC. It showed a protonated molecular ion at *m/z* 442, 112 Da higher than the parent drug, suggesting that it was a conjugate. CAD product ion spectrum of *m/z* 442 gave an ion at *m/z* 362, loss of 80 Da (characteristic loss of SO_3) from the precursor ion, indicating that it was a sulfate. Treatment of the urine sample with β-glucuronidase/aryl sulfatase resulted in the disappearance of **M11**, further suggesting that **M11** was a sulfate conjugate. The other ion at *m/z* 138 suggested the presence of a hydroxyl group on the pyrimidine ring. The significant and distinct ion at *m/z* 245, loss of 117 Da (succinimide + H_2O) from

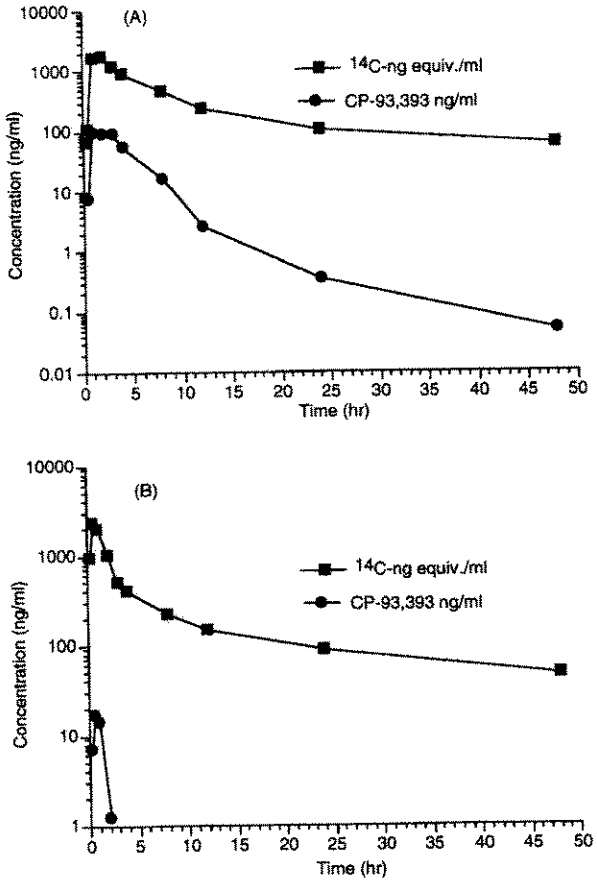

FIG. 8. *Mean plasma concentration-time curves of total radioactivity and unchanged CP-93,393 in (A) male (N = 2) and (B) female monkeys (N = 2).*

the ion at *m/z* 362, suggested that the oxidation had occurred at the pyrido-pyrazinyl-methyl part of the molecule (fig. 6*A*). Based on these data, **M11** was tentatively identified as a sulfate conjugate of the hydroxy[1-(2-{5-hydroxy-pyrimidin-2-yl}-octahydro-pyrido-[1,2-a]pyrazin7-yl)-methyl]-pyrrolidine-2,5-dione.

Metabolite M24. **M24** had a retention time of 20:52 min on HPLC and was found in all excreta. It showed a protonated molecular ion at *m/z* 362, 32 Da higher than the parent drug, suggesting that two oxygen atoms had been added to the molecule. MS/MS spectrum of **M24** showed ions at *m/z* 344, 245, 165, 138, and 108, similar to those obtained from the aglycone of **M11** (fig. 6*B*). **M24** was tentatively identified as hydroxy-[1-(2-{5-hydroxy-pyrimidin-2-yl}-octahydro-pyrido[1,2-a]pyrazin-7-yl)-hydroxymethyl]-pyrrolidine-2,5-dione.

Metabolite M13. **M13** had a retention time of 22:28 min on HPLC. It showed a protonated molecular ion at *m/z* 426, 80 Da higher than the hydroxylated CP-93,393, indicating that it was a conjugate. Treatment of urine with β-glucuronidase/aryl sulfatase resulted in the disappearance of **M13,** further suggesting that **M13** was a sulfate conjugate. **M13** had similar retention time and MS/MS spectrum to that of metabolite **M13** observed in rat (7). **M13** was thus identified as sulfate conjugate of 5-hydroxy-CP-93,393.

Metabolite M25. **M25** had a retention time of 23:33 min on HPLC and was present in urine, feces, and bile. It showed a protonated molecular ion at *m/z* 456, 126 Da higher than the parent drug, indicating that it was a conjugate. The CAD product ion spectrum of *m/z* 456 showed an ion at *m/z* 376, loss of 80 Da from the protonated molecular ion, suggesting the presence of a sulfate conjugate. Treatment of urine with aryl sulfatase resulted in the disappearance of **M25,** further suggesting that **M25** was a sulfate conjugate. The prominent fragment ions at *m/z* 209 and 235 indicated that the succinimide portion of the molecule was unsubstituted. The ions at *m/z* 168 and 182, 46 (16+30) Da higher than those of the parent drug, suggested the presence of a hydroxyl group and a *O*-methyl group at the pyrimidine ring (fig. 7*A*). Based on these data, **M25** was tentatively identified as the sulfate conjugate of methoxy-5-hydroxy-CP-93,393.

Metabolite M26. **M26** was present only in feces. It showed a protonated molecular ion at *m/z* 376, 46 Da higher than the parent drug, suggesting the addition of an oxygen atom and a methoxy group. The CAD product ion spectrum of *m/z* 376 showed ions at *m/z* 209, 235, 182, and 168 (fig. 7*B*). The ions at *m/z* 209 and 235 indicated that the succinimide portion of the molecule was unsubstituted. The fragment ion at *m/z* 168 and 182 suggested the presence of a hydroxyl group and a methoxy group at the pyrimidine ring. Based on these data, **M26** was tentatively identified as methoxy-5-hydroxy-CP-93,393.

Metabolite M15. **M15** had a retention time of 24:04 min on HPLC and was present in all excreta. It showed a protonated molecular ion at *m/z* 346, 16 Da higher than the drug, suggesting that it was a mono oxidation product of CP-93,393. It had same retention time as synthetic 5-hydroxy-CP-93,393 on HPLC and had an identical MS/MS spectrum. **M15** was thus identified as 5-hydroxy-CP-93,393.

Parent Drug. The parent drug had a retention time of 27:42 min. It showed a protonated molecular ion at *m/z* 330, the same as the parent drug. It had same retention time as synthetic CP-93,393 standard on HPLC and was thus identified as unchanged drug.

Plasma Concentrations and Metabolite Profiles. The mean plasma concentration-time curves for CP-93,393 and total radioactivity are graphically depicted in fig. 8*A* and 8*B* for male and female monkeys, respectively. The pharmacokinetic parameters for total radioactivity and unchanged CP-93,393 are shown in table 3. Absorption of CP-93,393 was rapid in both male and female monkeys, as indicated by the early appearance of radioactivity in plasma after oral administration. The mean C_{max} of CP-93,393 was 143.2 ng/ml at 2.5 hr after the dose for male monkeys and 17.22 ng/ml at 0.4 hr after the dose for female monkeys. The mean C_{max} for total radioactivity were 2006.7 ng-equiv/ml and 2537.5 ng-equiv/ml for male and female monkeys, respectively.

Mean terminal phase $t_{1/2}$ and mean $AUC_{(0-\infty)}$ in male monkeys were 12.4 hr and 13732.6 ng-equiv·hr/ml, respectively, for total circulating radioactivity, and 4.2 hr and 497.7 ng·hr/ml, respectively, for the unchanged CP-93,393. Mean terminal phase $t_{1/2}$ and mean $AUC_{(0-\infty)}$ in female monkeys were 16.0 hr and 10310.7 ng·equiv/hr/ml, respectively, for total circulating radioactivity, and 0.32 hr and 13.7 ng·hr/ml, respectively, for the unchanged CP-93,393.

Unchanged CP-93,393 and a total of 10 radioactive peaks were detected in the HPLC-radiochromatogram from plasma of both male and female monkeys (not shown). The percentage of metabolites in relation to the total radioactivity extracted from the plasma of both male and female monkeys is presented in table 4. There were only minor qualitative differences in the metabolic profiles between male and female monkeys. However, the relative amount of unchanged CP-93,393 was much higher in the male monkeys than in the female monkeys. The metabolites were identified by ion spray LC/MS/MS using MRM technique and by comparisons of their retention times on HPLC with synthetic standards or metabolites observed in urine. MRM responses of plasma metabolites, **M23** (*m/z* 380→245), **M6** (*m/z* 364→138), **M18** (*m/z* 294→252), **M7** (*m/z* 522→346), **M8** (*m/z* 364→122), **M11** (*m/z* 442→245), **M24** (*m/z* 362→245), **M13** (*m/z* 426→346), **M25** (*m/z* 456→376), **M15** (*m/z* 346→138) and parent

TABLE 3

Pharmacokinetic parameters for total radioactivity in plasma of monkeys after oral administration of ^{14}C-CP-93,393 at a dose of 5 mg/kg

Animal No. CP-93,393 or Radioactivity	Pharmacokinetic Parameters				
	C_{max} (ng or ng-equiv/ml)	T_{max} (hr)	$AUC_{(0-\infty)}$ (ng or ng-equiv·hr/ml)	Kel (1/hr)	$t_{1/2}$ (hr)
Male 1					
CP-93,393	184.9	1.0	413.3	0.16	4.33
Radioactivity	2876.6	1.0	14329.9	0.055	12.49
CP-93,393 (%)	6.43		2.88		
Male 2					
CP-93,393	101.4	4.0	582.0	0.17	4.13
Radioactivity	1136.8	2.0	13135.2	0.056	12.33
CP-93,393 (%)	8.92		4.43		
Mean					
CP-93,393	143.2	2.5	497.7	0.17	4.23
Radioactivity	2006.7	1.5	13732.6	0.056	12.41
CP-93,393 (%)	7.13		3.62		
Female 1					
CP-93,393	10.7	0.25	9.9	2.62	0.26
Radioactivity	2860.2	0.5	11395.7	0.039	17.83
CP-93,393 (%)	0.38		0.09		
Female 2					
CP-93,393	23.7	0.50	17.4	1.80	0.38
Radioactivity	2214.8	1.0	9225.7	0.049	14.10
CP-93,393 (%)	1.07		0.19		
Mean					
CP-93,393	17.2	0.38	13.7	2.21	0.32
Radioactivity	2537.5	0.75	10310.7	0.044	15.97
CP-93,393 (%)	0.72		0.13		

TABLE 4

Percentages of metabolites of CP-93,393 in plasma of monkeys after oral administration of ^{14}C-CP-93,393 at a dose of 5 mg/kg

Metabolite No	% of Radioactivity in Plasma	
	Male*	Female*
M23	2.04	1.32
M6	0.88	1.35
M18+M7	17.29	16.70
M9	1.92	0.00
M8	0.54	0.2
M11	1.5	—
M24	5.65	1.21
M13	23.63	27.94
M25	—	0.13
M15	37.15	49.12
Parent drug	5.95	<0.5
	96.55	97.97

* Average of two animals.

drug (*m/z* 330→122) from male monkeys are shown in fig. 9. The MRM responses of metabolites from female monkeys plasma were similar to those of male monkeys. The tentatively identified metabolites accounted for >97% of the total radioactivity present in plasma of male and female monkeys. All of these metabolites were also identified in urine.

***In Vitro* Metabolites Profile.** The radio-HPLC profile of metabolites from monkey liver microsomal incubations is shown in fig. 10. CP-93,393 and a total of six radioactive peaks were detected in the chromatogram. The structures of metabolites were elucidated by LC/MS/MS analysis and confirmed by comparisons of their retention times on HPLC with synthetic standards. SIM responses of four oxidative metabolites (**M6**, **M18**, **M9**, **M15**) and parent drug are shown in fig. 11. Thus, the major *in vivo* oxidative metabolites were also observed *in vitro*.

Discussion

After oral administration of ^{14}C-CP-93,393 to bile cannulated cynomolgus monkeys, radioactivity was rapidly absorbed and eliminated into urine, bile, and feces with the majority of the dose being accounted for within 48 hr after the dose. The excretion of the majority (61–86%, table 1) of the total radioactivity in urine and bile was indicative of excellent absorption from the gastrointestinal tract. Unlike rats, the major portion of the administered radioactivity was recovered in urine, indicating that the urinary excretion was the primary route of elimination of CP-93,393 and its metabolites in monkey (7).

At the time of C_{max}, the majority of the radioactivity in plasma was comprised of metabolites, and only a small percentage of administered radioactivity was excreted as unchanged drug in urine. The major portion of radioactivity recovered in urine was excreted as the conjugates of hydroxylated metabolites. A total of 15 metabolites in urine, 11 metabolites in bile, and 13 metabolites in feces of cynomolgus monkeys were identified by ion spray LC/MS/MS. The use of ion spray, a very soft ionization technique, has allowed the identification of both phase I and polar phase II metabolites (7, 18). The plausible scheme for the biotransformation pathways of CP-93,393 in monkey is shown in fig. 12. One of the major routes of metabolism involved oxidation on the pyrimidine ring followed by conjugation with glucuronic acid and sulfuric acid (**M7**, **M13**, and **M15**) similar to that observed for rat (7), and other structurally related drugs (19–21). The exact position of the hydroxyl group was determined by comparing the retention time with a synthetic standard. Metabolite **M15** was

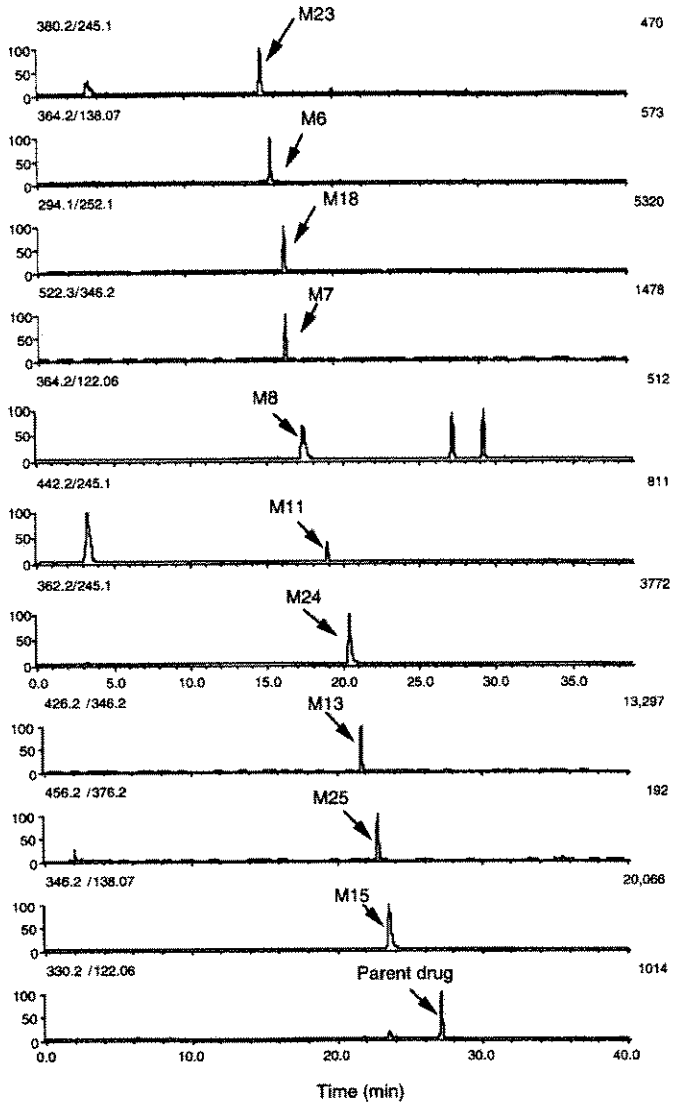

FIG. 9. *Reconstructed MRM responses of CP-93,393 metabolites in plasma.*

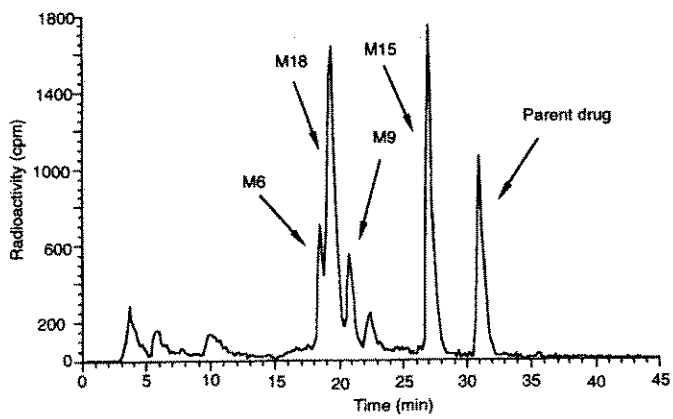

FIG. 10. *HPLC-radiochromatogram of* in vitro *metabolites of CP-93,393 from monkey liver microsomes.*

found to undergo further metabolism in monkey by oxidation at the 5-hydroxy-pyrimidine ring and subsequent methylation of the resulting catechol intermediate, presumably by catechol-*O*-methyl transferase to form metabolite **M26**. In urine and bile **M26** was excreted as

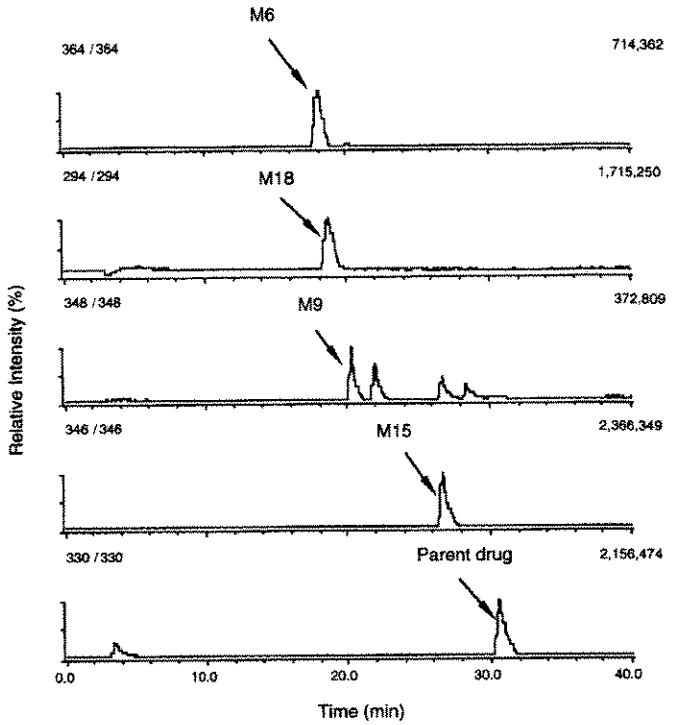

FIG. 11. *SIM chromatograms of* in vitro *metabolites of CP-93,393 from monkey liver microsomes.*

glucuronide conjugate (**M25**), whereas in feces it was recovered as aglycone, possibly because of hydrolysis of glucuronide conjugate by gut microflora (22). The combined metabolites obtained from aromatic hydroxylation pathway accounted for 38–47% of the dose in excreta. The other metabolites were caused by hydrolysis of the succinimide ring (**M6**, **M9**, **M19**, **M22**, and **M23**) and oxidation at the pyrido-pyrazine-methyl moiety (**M11**), similar to those found in rats. However, in contrast to rats, the oxidation at the succinimide ring was a minor metabolic pathway in monkeys (7).

In the present study, a number of novel metabolites (**M18**, **M20**, and **M21**) of CP-93,393 were identified. These metabolites resulted from the oxidative degradation of the pyrimidine ring. The splitting of an imidazolidine ring (23, 24) and, recently, the cleavage of pyridine ring has been reported (25). LC/MS analysis of **M18** suggested the protonated molecular ion at *m/z* 294, 42 Da higher than the *N*-despyrimidinyl-CP-93,393. Based on addition of 42 Da to the pyridopyrazinyl part of the molecule, two structures were originally considered for **M18**: *N*-acetyl conjugate of the *N*-despyrimidinyl CP-93,393 and oxidative degradation of the pyrimidine ring to form the amidine analog (fig. 13). *N*-acetyl conjugates of few drugs containing an arylpiperazine or a pyridinyl-piperazine moiety have been reported (26–28), and it has been suggested that prior hydroxylation occurred in the para position of the aryl ring with respect to piperazinyl nitrogen and was followed by formation of an unstable quinone intermediate culminating in cleavage between the aryl ring and nitrogen of the piperazine ring (27). *N*-Dearylated product then undergoes phase II metabolism by *N*-acetylation (26–28). Because 5-hydroxylation was the major metabolic pathway for CP-93,393, the formation of an *N*-acetyl conjugate of the *N*-desprimidiny-CP-93,393 was possible. However, the intermediate, *N*-desprimidinyl-CP-93,393, was not detected, as such, *in vivo*.

In an attempt to differentiate between these two isomeric structures of **M18** (fig. 13), CP-93,393 was incubated with monkey liver microsomes. Surprisingly **M18**, but not *N*-despyrimidinyl-CP-93,393, was

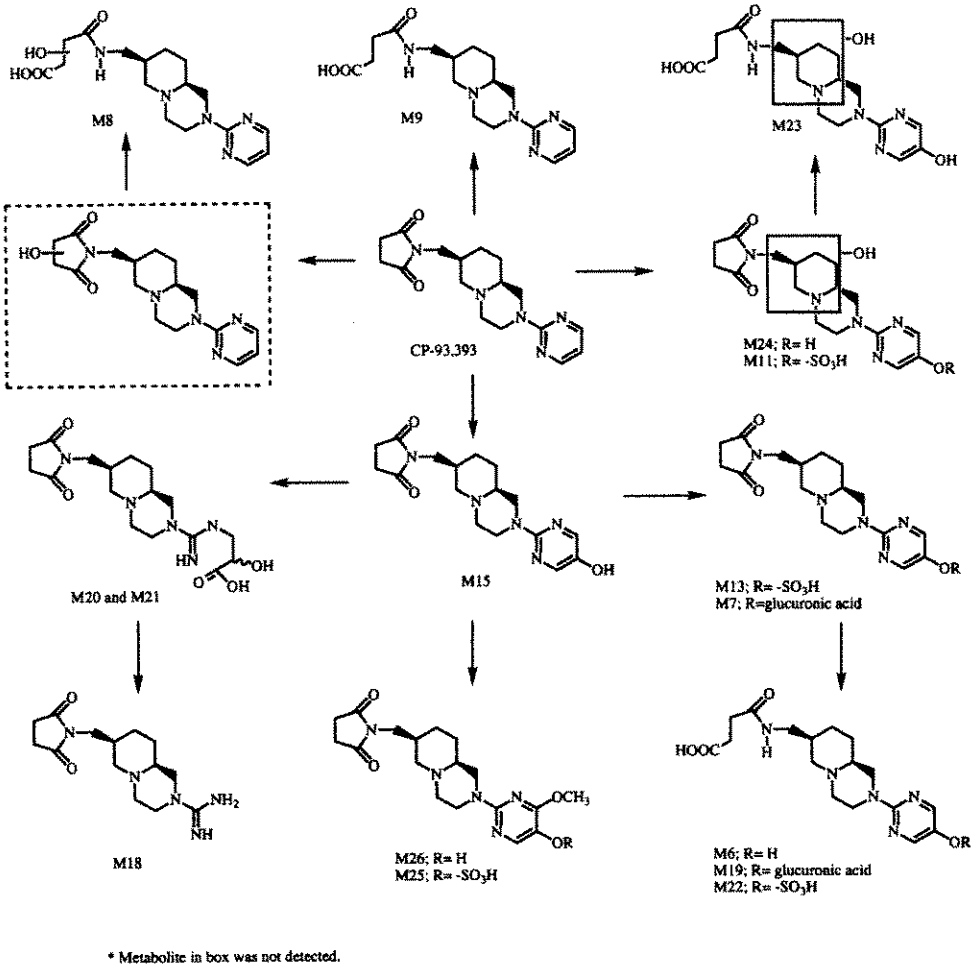

FIG. 12. *Biotransformation pathways for CP-93,393 metabolism in monkey.*

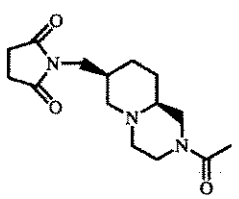

N-acetyl-N-despyrimidinyl

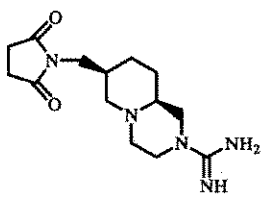

Carboxamidine

FIG. 13. *Possible structures of metabolite* **M18**.

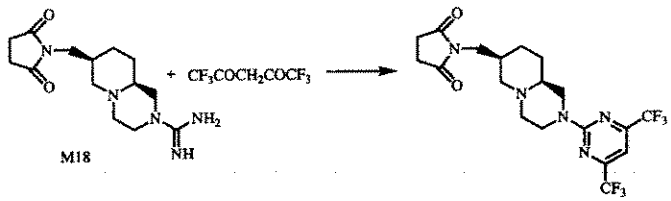

FIG. 14. *Derivatization of* **M18** with hexafluoroacetylacetone.

detected in microsomal incubations. These data suggested that **M18** was an oxidative metabolite, *N*-despyrimidinyl-amidine derivative, rather than a *N*-acetyl conjugate of *N*-despyrimidinyl-CP-93,393. The structure of **M18** as the carboxamidine analog was further confirmed by treatment with hexafluoroacetylacetone which resulted in the formation of bis-trifluoromethyl-CP-93,393 (fig. 14), a characteristic reaction for the detection of carboxamidines (13). The mechanism for the formation of this novel metabolite is not known at this time. Metabolite **M24** detected in urine and feces seems to be formed by further oxidation of **M15**. The oxidative metabolite **M24** was found to undergo subsequent hydrolysis of the succinimide ring (**M23**) or conjugation with sulfuric acid (**M11**). Metabolite **M11** and **M23** were present in urine and feces only, whereas **M24** was present in bile as well. The MS/MS spectrum of **M24** showed a significant and distinct ion at *m/z* 245, loss of 117 Da (succinimide + H_2O) from the molecular ion, suggesting that the oxidation had occurred at the pyrido-pyrazinyl-methyl part of the molecule. Two possible sites for such oxidation are: oxidation alpha to the nitrogen of either the succinimide ring or the pyrido-pyrazine ring to form carbinolamines. Stable carbinolamine intermediates have been reported for several drugs, including hexamethylmelamine (29), carbamates (30), and methylxanthines (31). Attempts to further characterize these metabolites were unsuccessful. Therefore, metabolites **M11**, **M23**, and **M24** were only partially identified.

The metabolic profile of pooled plasma (0–24 hr) from both male and female monkeys showed no significant qualitative differences. The 5-hydroxy metabolite, **M15** (37–49%), its sulfate and glucuronide conjugates (**M7** and **M13**, ~34%), and the pyrimidine cleaved product (**M18**, ~8%) were identified as major circulating metabolites in both male and female monkeys. The other metabolite **M9**, a hydrolysis product of CP-93,393, was present in smaller amount in male monkeys.

In summary, CP-93,393 is well absorbed and extensively metabolized in monkey. In addition to hydroxylation of the pyrimidine ring and hydrolysis of the succinimide ring, a novel metabolic pathway was identified. The identification of these metabolic pathways of CP-93,393 will broaden our understanding of the metabolism of other pyrimidinyl-piperazine drugs. The identified metabolites accounted for approximately 90, 93, 97, and 92% of the total radioactivity present in urine, bile, plasma, and feces, respectively.

Acknowledgments. We would like to thank Drs. Keith McCarthy, Kathleen Zandi, and Mike Bright for providing radiolabeled CP-93,393 and synthetic standards; Ms. Beth Obach and Mr. Victor Soliman for technical assistance; Dr. Mark Kovacs for performing the surgical procedures; Dr. Donald Tweedie for providing monkey liver microsomes; and Drs. Jim Baxter, Hassan Fouda, and Robert Ronfeld for helpful suggestions.

References

1. A. W. Schmidt, C. B. Fox, J. Lazzaro, S. McLean, A. Ganong, D. W. Schulz, K. Desai, G. M. Bright, and J. Heym: CP-93,393, a novel anxiolytic-antidepressant agent with both 5-HT1A agonist and alpha-2 adrenergic properties: *in vitro* studies. *Neurosci. Abstr.* **21,** 2106 (1995).
2. L. S. Reynolds, J. P. Braselton, J. S. Sprouse, H. Rollema, T. Clarke, S. McLean, W. Horner, and J. Heym: *In vivo* profile of CP-93,393: evidence of combined 5-HT1A agonist and alpha-2 adrenergic antagonist activities. *Neurosci. Abstr.* **21,** 2106 (1995).
3. P. A. Seymour, K. Desai, and G. M. Bright: Anxiolytic activity of CP-93,393: enhanced efficacy via combined 5-HT1A agonist and alpha-2 adrenergic antagonist activities. *Neurosci. Abstr.* **21,** 2106 (1995).
4. A. W. Schmidt, C. B. Fox, E. R. Jackson, J. Lazzaro, S. McLean, A. Ganong, S. H. Zorn, D. W. Schulz, K. Desai, G. M. Bright, and J. Heym: CP-93,393, *in vitro* characterization of a novel anxiolytic/antidepressant agent with both 5-HT1A agonist and alpha-2 adrenergic properties. *J. Neurochem.* **66(Suppl. 2),** S-38 (1996).
5. W. P. Weisenburger, C. L. Kozak, L. A. Medeiros, and D. S. Chapman: Evaluation of a new anxiolytic and antidepressant, CP-93, 393: pre- and post natal study in rats. *Teratology* **53,** 123 (1996).
6. H. Rollema, T. Clarke, Y. Lu, A. W. Schmidt, and J. S. Sprouse: Comparison of the effects of CP-93,393 and buspirone on 5HT and NE release: microdialysis studies in the hippocampus of freely moving rat and guinea pig. *J. Neurochem.* **66(Suppl. 2),** S-37 (1996).
7. C. Prakash and V. Soliman: Metabolism and excretion of a novel anti-anxiety drug candidate, CP-93,393 in Long Evans rats: differentiation of regioisomeric glucuronides by LC/MS/MS and LC/MS/MS/MS. *Drug Metab. Dispos.* **25,** 1288–1297 (1997).
8. E. L. Luther, M. J. Cole, V. Soliman, J. G. Baxter, and H. G. Fouda: HPLC/RAM/ESI/MS/MS studies on the metabolic fate of the anxiolytic agent CP-93,393. In "Proceedings of the 44th American Society of Mass Spectrometry Conference on Mass Spectrometry and Allied Topics," Portland, OR (Abstr.), p. 250, 1996.
9. T. Poll, A. F. Abdel Hady, R. Karge, G. Linz, J. Weetman, and G. Helmchen: *N*-substituted hydroxysuccinimide from (*S*) malic acid as a new reagents for asymmetric Diels-Alder additions to enoates. *Tetrahedron Lett.* **30,** 5595–5598 (1989).
10. H. Shih and G. O. Rankin: Convenient synthesis of *N*-aryl-2-hydroxysuccinimides and characterization of their hydrolysis products. *Synthesis* 866–867 (1989).
11. M. J. Avery and H. G. Fouda: Quantitative determination of CP-93,393 in serum at trace levels by HPLC/MS/MS. In "Proceedings of the 44th American Society of Mass Spectrometry Conference on Mass Spectrometry and Allied Topics," Portland, OR (Abstr.), p. 1311, 1996.
12. M. Rowland and T. N. Tozer: In "Clinical Pharmacokinetic Concepts and Applications," 2nd ed. Lea and Febiger, Philadelphia, 1989.
13. S. L. Malcolm and T. R. Marten: Determination of debrisoquine and its 4-hydroxy metabolite in plasma by gas chromatography/mass spectrometry. *Anal. Chem.* **48,** 807–809 (1976).
14. D. J. Tweedie and M. D. Burke: Differential effects of phenobarbitone and 3-methylcholanthrene induction on the hepatic microsomal metabolism of the beta-carbolines harmine and harmol. *Biochem. Pharmacol.* **32,** 653–63 (1983).
15. P. K. Smith, R. I. Krohn, G. T. Hermanson, A. K. Mallia, F. H. Gartner, M. D. Provenzano, E. K. Fujimoto, N. M. Goeke, B. J. Olson, and D. C. Klenk: Measurement of protein using bicinchoninic acid. *Anal. Biochem.* **150,** 76–85 (1985).
16. T. Omura and R. Sato: The carbon monoxide binding pigment of liver microsomes: I. Evidence of its hemoprotein nature. *J. Biol Chem.* **239,** 2370–78 (1964).
17. C. Prakash, A. Kamel, W. Anderson, and H. Howard: Metabolism and excretion of the antipsychotic drug ziprasidone in the rat after administration of a mixture of ^{14}C- and ^{3}H labeled ziprasidone. *Drug Metab. Dispos.* **25,** 212–218 (1997).
18. C. Prakash, A Kamel, J. Gummerus, and K. Wilner: Metabolism and excretion of the antipsychotic drug ziprasidone in human. *Drug Metab. Dispos.* **25,** 863–872 (1997).
19. H. K. Jajoo, R. F. Mayol, J. A. Labudde, and I. A. Blair: Metabolism of the antianxiety drug buspirone in the rat. *Drug Metab. Dispos.* **17,** 625–633 (1989).
20. H. K. Jajoo, R. F. Mayol, J. A. Labudde, and I. A. Blair: Metabolism of the antianxiety drug buspirone in human subjects. *Drug Metab. Dispos.* **17,** 634–640 (1989).
21. Y. Mizuno, K. Matoba, I. Nakatsuka, and A. Yoshtake: Metabolism of SM-3997. *Clin. Rep.* **26,** 209–225 (1992).
22. M. A. Shamat: The role of gastrointestinal microflora in the metabolism of drugs. *Int. J. Pharmaceut.* **97,** 1–13 (1993).
23. P. Koch, D. R. Hirst, and B. R. Wartburg: Biological fate of sirdalud in animals and man. *Xenobiotica* **19,** 1255–1265 (1989).
24. M. Fujimaki, N. Ishigaki, and H. Hakusui: Metabolic fate of the oral hypoglycaemic agent, midaglizole, in rats. *Xenobiotica* **19,** 609–625 (1989).
25. M. Chang, V. K. Sood, G. J. Wilson, D. A. Kloosterman, P. E. Sanders, M. J. Hauer, and P. E. Fagerness: Metabolism of the human immunodefficiency virus type 1 reverse transcriptase inhibitor delavirdine in rats. *Drug Metab. Dispos.* **25,** 228–242 (1997).
26. A. Enreille, J. F. Pognat, M. J.Galmier, C. Lartigue-Mattei, J. L. Chabard, N. Busch, and J. A.Berger: *N*-Dephenylated and *N*-phenyl urinary metabolites of mociprazine (CERM 3517) in beagle dogs after oral administration: a mass spectrometric determination. *Eur. J. Drug Metab. Pharmacokinet.* **16,** 161–172 (1991).
27. T. Ohe, T. Mashino, and M. Hirobe: Novel metabolic pathway of arylethers by cytochrome P450: cleavage of the oxygen-aromatic ring bond accompanying ipso-substitution by the oxygen atom of the active species in cytochrome P450 models and cytochrome P450. *Archiv. Biochem. Biophy.* **310,** 402–409 (1994).
28. Y. C. Chui, B. Esaw, and B. Laviolette: Investigation of the metabolism of azaperone in the horse. *J. Chromatogr.* **652,** 23–33 (1994).
29. A. Gescher, M. D'Incalci, R. Fanelli, and P. Ferina: *N*-Hydroxymethylpentamethylmelamine, a major *in vitro* metabolite of hexamethylmelamine. *Life Sci. (Washington, D.C.)* **26,** 147–154 (1980).
30. G. Huizing, J. Segura, and A. H. Beckett: On the mechanism of metabolic N-dealkylation. Isolation of relatively stable carbinolamine. *J. Pharm. Pharmacol.* **32,** 650–651 (1980).
31. N. Lander, A. H. Soloway, J. P. Minton, B. D. Rawal, and C. C. Gairola: Potential metabolite mutagens of caffeine and various methylxanthines. *J. Pharm. Sci.* **77,** 955–958 (1988).